



Published in final edited form as:

Cell Rep. 2022 September 13; 40(11): 111345. doi:10.1016/j.celrep.2022.111345.

Pak2-mediated phosphorylation promotes ROR γ t ubiquitination and inhibits colonic inflammation

Mahesh Kathania^{1,2,3}, Ritesh Kumar^{1,2,3}, Elviche Taskem Lenou^{1,2,3}, Venkatesha Basrur⁴, Arianne L. Theiss⁵, Jonathan Chernoff⁶, K. Venuprasad^{1,2,3,7,*}

¹Department of Internal Medicine, UT Southwestern Medical Center, Dallas, TX 75390, USA

²Department of Immunology, UT Southwestern Medical Center, Dallas, TX 75390, USA

³Harold C. Simmons Comprehensive Cancer Center, UT Southwestern Medical Center, Dallas, TX 75390, USA

⁴Department of Pathology, University of Michigan, Ann Arbor, MI 48109, USA

⁵University of Colorado, School of Medicine, Division of Gastroenterology and Hepatology, Anschutz Medical Campus, Aurora, CO, USA

⁶Cancer Signaling and Epigenetics Program, Fox Chase Cancer Center, Philadelphia, PA, USA

⁷Lead contact

SUMMARY

Dysregulated interleukin-17 (IL-17) expression and its downstream signaling is strongly linked to inflammatory bowel diseases (IBDs). However, the molecular mechanisms by which the function of ROR γ t, the transcription factor of IL-17, is regulated remains elusive. By a mass spectrometry-based approach, we identify that Pak2, a serine (S)/threonine (T) kinase, directly associates with ROR γ t. Pak2 recognizes a conserved KRLS motif within ROR γ t and phosphorylates the S-316 within this motif. Genetic deletion of Pak2 in Th17 cells reduces ROR γ t phosphorylation, increases IL-17 expression, and induces severe colitis upon adoptive transfer to *Rag1*^{-/-} mice. Similarly, reconstitution of ROR γ t-S316A mutant in *Rorc*^{-/-} Th17 cells enhances IL-17 expression and colitis severity. Mechanistically, we demonstrate that Pak2-mediated phosphorylation causes a conformational change resulting in exposure of the ubiquitin

This is an open access article under the CC BY-NC-ND license (<http://creativecommons.org/licenses/by-nc-nd/4.0/>).

*Correspondence: venuprasad.poojary@utsouthwestern.edu.

AUTHOR CONTRIBUTIONS

M.K., R.K., and T.L.E. performed the experiments, analyzed the data, and helped to prepare the manuscript. V.B. performed MS analysis. A.L.T. and J.C. helped to prepare the manuscript. K.V. conceived the project, designed the experiments, and wrote the manuscript.

SUPPLEMENTAL INFORMATION

Supplemental information can be found online at <https://doi.org/10.1016/j.celrep.2022.111345>.

DECLARATION OF INTERESTS

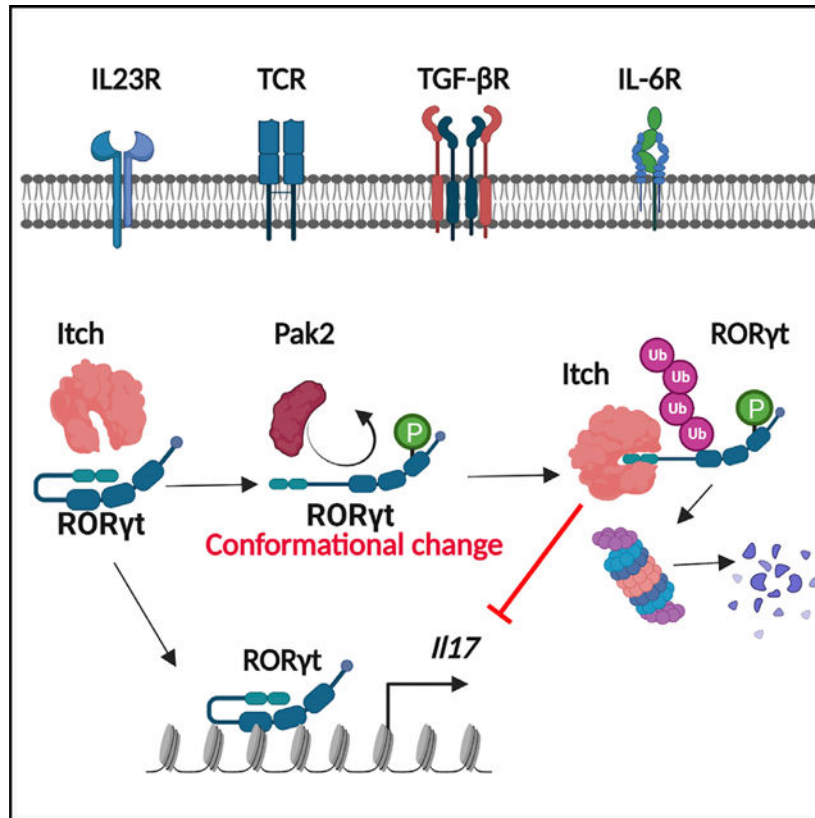
The authors declare no competing interests.

INCLUSION AND DIVERSITY

We worked to ensure sex balance in the selection of non-human subjects. One or more of the authors of this paper self identifies as an underrepresented ethnic minority in science.

ligase Itch interacting PPLY motif and degradation of ROR γ t. Thus, we have uncovered a mechanism by which the activity of ROR γ t is regulated that can be exploited therapeutically.

Graphical Abstract



In brief

Kathania et al. show that Pak2, a Ser/Thr kinase, associates with ROR γ t and phosphorylates Ser-316 of ROR γ t. Deletion of Pak2 in Th17 cells enhances IL-17 expression and colitis severity. Pak2-mediated phosphorylation causes a conformational change resulting in increased ubiquitination of ROR γ t by the E3 ubiquitin ligase Itch.

INTRODUCTION

Interleukin-17 (IL-17) is a proinflammatory cytokine that is produced by a variety of immune cells, including the Th17 subset of helper CD4⁺ T cells, δ T cells, and innate lymphoid cells (Honda and Littman, 2016; Kumar et al., 2021b; Zhou and Sonnenberg, 2020). IL-17 signals through the IL-17 receptor, composed of IL-17RA and IL-17RC receptor subunits (Gaffen, 2009). The binding of IL-17 to its receptor activates the target cells, such as epithelial cells, endothelial cells, and fibroblasts, and induces the expression of CXCL1, CXCL2, and CXCL8, which attract myeloid cells such as neutrophils and promote inflammation (Gaffen, 2009). IL-17 is critically essential for host defense against fungal and bacterial infections. However, dysregulated IL-17 expression and downstream

signaling are involved in several human diseases, including inflammatory bowel disease (IBD) (McGeachy et al., 2019; Patel and Kuchroo, 2015).

The orphan nuclear receptor ROR γ t is a transcription factor crucial for IL-17 expression (Ivanov et al., 2006; Zhang et al., 2008). ROR γ t consists of a ligand-independent activation function 1 helix, a DNA-binding domain, a flexible hinge domain, and a C-terminal ligand-binding domain (Kumar et al., 2021b). The zinc finger motifs within the DNA-binding domain recognize the ROR response elements within the IL-17 promoter to induce IL-17 expression (Kumar et al., 2021b). Given the critical role of IL-17 in inflammatory diseases, ROR γ t has emerged as an attractive target for pharmacological interventions (Beringer et al., 2016). However, a clear understanding of the regulation of ROR γ t is currently lacking, which is absolutely necessary to target ROR γ t effectively.

Crosstalk between different posttranslational modifications plays a critical role in regulating the activity of transcription factors (Hunter, 2007). We have demonstrated earlier that the E3 ligase Itch targets ROR γ t for ubiquitination, and Itch deficiency results in spontaneous rectal prolapse as a result of severe spontaneous colitis (Kathania et al., 2016). Here, we show how Pak2-mediated phosphorylation facilitates ROR γ t ubiquitination to prevent excessive Th17 response. A clear understanding of this regulatory pathway could lead to the development of safe and highly selective modulators of ROR γ t as a targeting strategy for inflammatory diseases driven by IL-17.

RESULTS

Pak2 interacts and phosphorylates ROR γ t

To gain molecular insights into the regulation of ROR γ t, we immunoprecipitated ROR γ t from the cell lysate of *in vitro*-generated Th17 cells and subjected it to mass spectrometry (MS) analysis. Through this approach, we identified Pak2 as a ROR γ t-binding protein (Figures 1A and S1A). We also precipitated ROR γ t from the cell lysate of CD4⁺ T cells sorted from colonic lamina propria lymphocytes (cLPLs) of mice treated with DSS and subjected it to MS analysis and found Pak2 as a ROR γ t-binding protein (Figure S1B). To validate the MS results, we transiently transfected 293T cells with plasmids encoding Myc-tagged Pak2 and FLAG-tagged ROR γ t. Cell lysates were immunoprecipitated with either anti-FLAG or anti-Myc antibodies. Samples immunoprecipitated with the anti-Myc antibody contained FLAG-ROR γ t, and vice versa (Figure S1C), suggesting that Pak2 and ROR γ t physically interact with each other. To determine whether this interaction occurred between endogenous proteins in primary cells, we performed immunoprecipitation assays with anti-Pak2 and anti-ROR γ t antibodies using the lysate of *in vitro*-generated Th17 cells and found an interaction between ROR γ t and Pak2 (Figure 1B). Similar results were obtained in CD4⁺ T cells sorted from cLPLs of mice treated with DSS (Figure S1D). We also performed glutathione S-transferase (GST) pull-down assays using recombinant Pak2 protein. GST-ROR γ t, but not GST alone, precipitated recombinant Pak2 (Figure 1C), suggesting a direct interaction.

Pak2 is a Serine/Threonine protein kinase that phosphorylates its target proteins on KRX[S/T] motif (Taglieri et al., 2014). Amino acid sequence analysis revealed a highly

conserved KRLS motif in ROR γ t, which could be potentially phosphorylated (Figure 1D). To test if Pak2 phosphorylates ROR γ t, we knocked down Pak2 in *in vitro*-generated Th17 cells using short hairpin RNA (shRNA) lentiviral particles and found that inhibiting Pak2 reduced the phosphorylation of ROR γ t. As seen in Figure 1E, knocking down Pak2 reduced ROR γ t phosphorylation. Further, we confirmed that Pak2 phosphorylates ROR γ t by performing an *in vitro* kinase assay. As shown in Figure 1F, incubation of ROR γ t with wild-type Pak2, but not a Pak2 kinase-dead mutant (Pak2- K278R), resulted in ROR γ t phosphorylation. Similarly, incubation of the ROR γ t- S316A mutant with wild-type Pak2 exhibited a defect in phosphorylation. These data suggest that Pak2 phosphorylates ROR γ t at Serine 316 (S316). To further confirm these results, we reconstituted CD4⁺ T cells isolated from Pak2^{fl/fl}CD4^{Cre} mice with either wild-type Pak2 or Pak2- K278R by lentivirus transduction. We found ROR γ t phosphorylation in Pak2^{-/-} cells reconstituted with wild-type Pak2 but not the Pak2- K278R mutant (Figure 1G). Similarly, reconstitution of Rorc^{-/-} CD4⁺ T cells with wild type, but not the ROR γ t- S316A mutant, resulted in ROR γ t phosphorylation (Figure 1H). These data collectively indicate that Pak2 phosphorylates ROR γ t at S316 in Th17 cells.

Inhibition of Pak2 enhances IL-17 expression and colitis

To gain insights into the functional consequence of Pak2-mediated phosphorylation of ROR γ t, we analyzed the expression of *Il17a* and *Il17f* mRNA in *in vitro*-generated Th17 cells from wild-type and Pak2^{fl/fl}CD4^{Cre} mice. Results of real-time PCR experiments showed that Pak2 deficiency enhances the expression of *Il17a* and *Il17f* (Figures S2A and S2B). However, no significant difference in *Rorc* mRNA level was observed (Figure S2C). To gain *in vivo* evidence for Pak2-mediated phosphorylation of ROR γ t in colonic inflammation, we sorted CD4⁺ T cells from wild-type and Pak2^{fl/fl}CD4^{Cre} mice, and the cells were differentiated under Th17 polarizing conditions. The cells were then adoptively transferred into *Rag1*^{-/-} mice as described before (Lee et al., 2009). The *Rag1*^{-/-} mice that received Pak2^{-/-} Th17 cells showed more body weight loss, an increased fecal occult blood (FOB) score, increased diarrhea, splenomegaly, reduced colon length, and a higher weight-to-length ratio of the colon compared with the mice that received wild-type Th17 cells (Figures 2A–2E). Colonoscopic examination showed increased inflammation in mice that received Pak2^{-/-} Th17 cells compared with those that received wild-type Th17 cells (Figures 2F and 2G). Similarly, histo-logical analysis of H&E-stained sections showed greater infiltration of inflammatory cells, more crypt damage, and higher clinical scores in mice that received Pak2^{-/-} Th17 cells than wild-type cells (Figures 2H and 2I). Real-time PCR analysis showed higher expression of *Il17a* and *Il17f* mRNA in the colonic mucosa of mice that received Pak2^{-/-} Th17 cells (Figures 2M and 2N). Further, flow cytometric analysis (Figure S2D) showed an increased IL-17 expression by the adoptively transferred Pak2^{-/-} Th17 cells in *Rag1*^{-/-} mice compared with wild-type Th17 cells (Figure 2J). However, no significant changes in interferon gamma (IFN- γ) production (Figures 2K and S2E) was observed. Also, as expected, no change in IL-17 expression by innate lymphoid cells (ILCs) of host *Rag1*^{-/-} mice was observed (Figure 2L). These data suggest that Pak2-mediated phosphorylation in Th17 cells plays a crucial role in colonic inflammation.

To test if increased IL-17 expression by the adoptively transferred *Pak2*^{-/-} Th17 cells is potentially due to elevated *Rorc* mRNA expression, we performed real-time PCR analysis. No change in *Rorc* mRNA level (Figure 2O) was noted. However, immunoblotting the lysate of cLPLs showed an increased level of ROR γ t protein in mice that received *Pak2*^{-/-} Th17 cells compared with wild-type Th17 cells (Figure 2P). These data suggest that Pak2 regulates ROR γ t protein turnover without affecting ROR γ t transcription.

Pak2 enhances the ubiquitination of ROR γ t

Next, we sought to investigate how Pak2 regulates ROR γ t protein turnover. We have previously shown that Itch targets ROR γ t for ubiquitination (Kathania et al., 2016). Since phosphorylation can affect protein turnover via ubiquitination (Hunter, 2007), we hypothesized that Pak2-mediated phosphorylation promotes ROR γ t ubiquitination. To test this hypothesis, we performed a ubiquitination assay by co-expressing either wild-type ROR γ t, ROR γ t- S316A kinase mutant, or ROR γ t- S316D phospho-mimetic mutants along with the Itch. Our results showed an increased polyubiquitination of ROR γ t- S316D (Figure 3A), suggesting that phosphorylation regulates ubiquitination of ROR γ t. To further confirm that phosphorylation promotes ROR γ t ubiquitination, we performed *in vitro* ubiquitin assays using recombinant wild-type ROR γ t or ROR γ t mutants (ROR γ t- S316A or ROR γ t- S316D) along with recombinant Itch. Increased ubiquitination of ROR γ t- S316D phospho-mimetic mutant was observed compared with the ROR γ t-DS-A phospho-null mutant (Figure 3B). Finally, we analyzed ubiquitination of ROR γ t in *in vitro*-generated Th17 cells from *Pak2*^{fl/fl}*CD4*^{Cre} mice lentivirally transduced with wild-type Pak2 or the Pak2- K278R kinase-dead mutant. We found an increased ubiquitination in the cells transduced with wild-type Pak2 compared with the Pak2- K278R kinase-dead mutant (Figure 3C).

To investigate if phosphorylation-regulated ubiquitination affected ROR γ t protein turnover, we performed a cycloheximide (CHX) chase experiment. The primary CD4⁺ T cells from *Rorc*^{-/-} mice were lentivirally transduced with wild-type ROR γ t and ROR γ t- S316D phospho-mimetic mutants. The cells were then treated with CHX, and the level of ROR γ t was analyzed by immunoblotting. Our results showed a reduced abundance of ROR γ t protein in ROR γ t- S316D compared with wild-type ROR γ t transduced cells (Figure 3D). Similarly, the CHX chase experiment in *in vitro*-generated Th17 cells from *Pak2*^{fl/fl}*CD4*^{Cre} mice reconstituted with wild-type Pak2 or the Pak2- K278R kinase-dead mutant also showed a reduced abundance of ROR γ t protein in wild-type Pak2 transduced cells compared with the Pak2- K278R kinase-dead mutant (Figure 3E). These results strongly suggested that phosphorylation increases ROR γ t protein turnover. Additionally, the mRNA-to-protein ratio of ROR γ t in *Rorc*^{-/-} CD4⁺ T cells reconstituted with wild-type ROR γ t and ROR γ t- S316D phospho-mimetic mutant was lower compared with wild-type-ROR γ t (Figure 3F).

Itch is a HECT type E3 ligase that contains four WW domains (each of which contains two conserved tryptophan residues), which recognizes proline-rich PPXY (P, proline; X, any amino acid; Y, tyrosine) motifs in its substrate proteins (Venuprasad et al., 2015). We showed earlier that Itch binds to the conserved PPLY motif on ROR γ t via its WW domain (Kathania et al., 2016). To gain molecular insights into the mechanism by which

phosphorylation at S316 promotes ROR γ t ubiquitination, we performed homology modeling of mouse ROR γ t. *In silico* analysis of the modeled structure showed that S316 made an H-bond (3.6 Å) with a side-chain amino group of asparagine (N) 253 of the neighboring α -helix and stabilized the ligand-binding domain (LBD) of ROR γ t, hence there was less accessibility of the PPLY motif (Figure 3G). We then substituted the S316 with phosphomimetic aspartic acid residues (D) 316, and the energy of the modeled structure was minimized after the substitution mutation. The modeled structure revealed that the H-bond interaction between S316 to N253 is abolished after phosphorylation of serine, suggesting that phosphorylation may provide increased accessibility of the PPLY motif of ROR γ t to Itch (Figure 3G). To validate the computational analysis, we performed a GST pull-down assay using purified wild-type Itch, GST-ROR γ t, GST-ROR γ t- S316A, and GST-ROR γ t- S316D mutants. Our results showed that Itch association with ROR γ t- S316D mutant was more prominent compared with GST-ROR γ t or GST-ROR γ t- S316A mutant (Figure 3H). These results suggest that phosphorylation enhances the binding affinity of Itch to ROR γ t.

Phosphorylation of ROR γ t inhibits IL-17 expression and colonic inflammation

To confirm that Pak2-mediated phosphorylation prevents excessive IL-17-mediated inflammation, we reconstituted *Rorc*^{-/-} CD4⁺ T cells with wild-type ROR γ t or ROR γ t- S316A or ROR γ t- S316D mutants. Cells were cultured under Th17 polarizing conditions, and expression of IL-17 was measured by real-time PCR. Our results showed an increased *Il17a* expression in *Rorc*^{-/-} cells expressing ROR γ t- S316A mutant compared with wild-type ROR γ t, whereas significantly reduced *Il17a* expression was observed in cells expressing ROR γ t- S316D mutant (Figure 3I). However, no significant difference in *Rorc* mRNA was observed (Figure S2F).

To investigate the physiological impact of ROR γ t phosphorylation on the regulation of IL-17-mediated inflammation *in vivo*, we utilized an adoptive transfer colitis model (Lee et al., 2009). We sorted CD4⁺CD25⁻ cells from *Rorc*^{-/-} mice and reconstituted them with either empty vector, wild-type ROR γ t, or ROR γ t- S316A or ROR γ t- S316D mutants. The cells were differentiated under Th17 polarizing conditions for 5 days, and 5×10^5 cells were adoptively transferred into *Rag1*^{-/-} mice (Figure 4A). The mice were monitored for signs of disease, including weight loss, FOB, and diarrhea. *Rag1*^{-/-} mice that received Th17 cells expressing a phosphorylation-deficient mutant, ROR γ t- S316A, exhibited greater loss of body weight, higher FOB, diarrhea scores, splenomegaly, reduced colon length, and a higher weight-to-length ratio of the colon compared with host mice that received Th17 cells expressing ROR γ t- S316D mutant and wild-type ROR γ t (Figures 4B–4F). Colonoscopic examination revealed enhanced inflammation in *Rag1*^{-/-} mice that received Th17 cells expressing ROR γ t- S316A mutant compared with ROR γ t- S316D mutant or wild-type ROR γ t (Figures 4G and 4H). Histological analysis of H&E-stained sections showed greater infiltration of inflammatory cells, more crypt damage, and higher clinical scores for *Rag1*^{-/-} mice that received ROR γ t- S-A mutant expressing cells compared with ROR γ t- S-D mutant or wild-type ROR γ t cells (Figures 4I and 4J). *Rag1*^{-/-} mice that received Th17 cells expressing ROR γ t- S316A mutant had higher expression of *Il17a* and *Il17f* mRNA in the colonic mucosa (Figure 4K). Similarly, flow cytometric analysis of cLPLs showed increased IL-17 expression in *Rag1*^{-/-} mice that received Th17 cells expressing the ROR γ t- S316A

mutant compared with cells expressing the ROR γ t- S316D mutant or wild-type ROR γ t. However, there was no change in IFN- γ production by adoptively transferred cells (Figure 4L and 4M). Further expression of IL-17-induced chemokines and MMPs *Cxcl1*, *Ccl2*, *Ccl7*, *Ccl20*, *Mmp1*, *Mmp2*, *Mmp3*, and *Mmp13* were significantly upregulated in *Rag1*^{-/-} mice that received Th17 cells expressing ROR γ t- S316A mutation (Figures 3A and 3B). To test the potential difference in *Rorc* gene expression in adoptively transferred Th17 cells expressing wild-type ROR γ t and ROR γ t mutants, we performed real-time PCR experiments using RNA isolated from cLPLs of *Rag1*^{-/-} mice. As shown in Figure 4K, no significant changes in *Rorc* mRNA expression were observed. However, immunoblotting the lysates with anti-V5 antibody showed increased ROR γ t protein expression of the ROR γ t- S316A mutant, suggesting a defect in turnover of ROR γ t protein (Figure 4N). Together, these findings suggest that Pak2-mediated phosphorylation of ROR γ t negatively regulates IL-17 expression and controls colonic inflammation.

DISCUSSION

Genome-wide association studies have highlighted the central role of the ROR γ t:IL-17 pathway in several human inflammatory diseases (Duerr et al., 2006; Lock et al., 2002; Parkes et al., 2013). Accordingly, the IL-17-inducing transcription factor ROR γ t has emerged as an attractive target for pharmacological interventions (Beringer et al., 2016). Our results show that Pak2-mediated phosphorylation of ROR γ t at S316 inhibits IL-17 expression by promoting ubiquitination of ROR γ t. *Pak2*^{-/-} Th17 cells are highly colitogenic due to elevated IL-17 expression. Similarly, transfer of Th17 cells expressing ROR γ t- S316A phospho mutant resulted in severe colitis, whereas the ROR γ t- S316D mutation that mimics the constitutively phosphorylated form of the ROR γ t mutant resulted in attenuated colitis in *Rag1*^{-/-} mice. Mechanistically, we demonstrated that S316 phosphorylation of ROR γ t enhances its interaction with Itch due to increased exposure of the E3 ligase Itch interacting PPLY motif. Our results could be exploited therapeutically to inhibit IL-17-mediated inflammation.

Pak2 was shown to be essential for maintaining regulatory T cell (Treg) stability and their suppressive function, and loss of Pak2, specifically in Tregs, resulted in defective Treg function (O'Hagan et al., 2017). Our data show that Pak2 plays a distinct role in Th17 cells by facilitating ROR γ t degradation to curb excessive IL-17-mediated inflammation. Adoptive transfer of Pak2-deficient Th17 cells into *Rag1*^{-/-} mice (which are devoid of T cells and Tregs) resulted in severe colitis. T cells recovered from the lamina propria of the recipient *Rag1*^{-/-} mice exhibited an increased level of ROR γ t protein. Similarly, adoptive transfer of Th17 cells expressing the ROR γ t- S316A phospho-null mutant resulted in a defect in ROR γ t protein turnover and elevated IL-17 expression. These data strongly suggest a distinct function for Pak2 in regulating Th17 cells and Tregs.

IL-17 is produced by a variety of immune cells, including Th17 cells, ILCs, Tc17 cells, natural killer (NK) cells, and neutrophils (Kumar et al., 2021b). The cell-surface receptors involved and the intracellular signaling pathways leading to the secretion of cytokines significantly differ in these cells. However, it remains poorly understood if different immune cells' regulation of IL-17 expression varies or adopts the same pathways. The data presented

here identify a previously unknown mechanism of regulation of the ROR γ t-IL-17 pathway by Pak2 in Th17 cells. Our assay systems exclude the regulation of other IL-17-producing cells such as NK cells, CD8⁺ T cells, and ILCs. If Pak2 regulates IL-17 expression in these cells by a similar mechanism remains unknown, which requires further detailed studies, including cell-type-specific knockout mice (e.g., NK cell or ILC-specific *Pak2*^{-/-} mice) and additional adoptive transfer experiments.

The upstream mechanisms that activate the Pak2-Itch pathway to trigger ROR γ t degradation in Th17 cells remain unclear. Pak2 is shown to be activated by Cdc42/Rac downstream of Vav following T cell receptor (TCR) stimulation (Ha et al., 2015; Taglieri et al., 2014). Therefore, it is possible that in Th17 cells, Pak2 acts as a feedback mechanism and inhibits IL-17 expression by phosphorylation of ROR γ t. It is also possible that IL-17R signaling activates Pak2 in Th17 cells to impede the pathogenicity of Th17 cells. Such a phenomenon has been reported recently via the induction of IL-24 (Chong et al., 2020). Additionally, Pak2 is involved in TGF- β signaling (Sato et al., 2013; Wilkes and Leof, 2006; Wilkes et al., 2003, 2005, 2009; Yan et al., 2012), which regulates Th17 development (Korn et al., 2009; Patel and Kuchroo, 2015). Therefore, it is also possible that Pak2 activated via the transforming growth factor β (TGF- β) pathway may trigger ROR γ t phosphorylation. Further, a detailed investigation of these pathways is essential to fully understand how ROR γ t protein turnover is regulated during an inflammatory response to prevent chronic inflammation.

The current strategies of targeting IL-17 using antagonistic antibodies (against IL-17 or its receptor) have shown some success in treating psoriasis and ankylosing spondylitis (Beringer et al., 2016); however, clinical trials using this approach led to mixed results in rheumatoid arthritis (RA) (Fragoulis et al., 2016; Genovese et al., 2013; Hueber et al., 2010) and failure in IBDs (Fitzpatrick, 2013; Hueber et al., 2012; Targan et al., 2016). Several recent studies have shown that ROR γ t function and protein stability are modified by posttranslational mechanisms, including ubiquitination, acetylation, and SUMOylation (Kumar et al., 2021b). A defect in ROR γ t protein degradation has been reported in tumor-infiltrated Th17 cells of patients with colorectal cancer (Sun et al., 2021). CRNDE-h protein was shown to form a complex with the PPLY region of ROR γ t, and binding of CRNDE-h to ROR γ t in patients' Th17 cells prevented ubiquitination and proteasomal degradation of ROR γ t by impeding its association with the Itch protein (Sun et al., 2021). On the contrary, our results show that Pak2 facilitates the binding of Itch to ROR γ t and promotes ROR γ t degradation. A clear understanding of the mechanism that regulates ROR γ t degradation could lead to alternative avenues to promote ROR γ t degradation at the site of inflammation. Such a strategy could transiently inhibit IL-17, resulting in therapeutic inhibition of Th17-mediated inflammation without deleterious effects observed in antibody-mediated systemic blocking of IL-17.

Limitations of the study

Although our study comprehensively shows that phosphorylation promotes ubiquitination of ROR γ t by enhancing its interaction with Itch, additional biophysical and cryoelectron microscopy evidence is necessary for the phosphorylation-dependent conformational

changes in ROR γ t. In our *in vivo* experiments, we have lentivirally expressed ROR γ t-S316A in CD4⁺T cells; studies using ROR γ t-S316A point mutation knockin mice will be necessary to determine the broader physiological relevance of our findings. Finally, in this study, we utilized only the Th17-adoptive transfer colitis model to demonstrate that phosphorylation of ROR γ t regulates Th17 cell-induced colon inflammation. If the Pak2-ROR γ t-Itch pathway operates in other Th17-dependent disease models needs to be tested.

STAR★METHODS

RESOURCE AVAILABILITY

Lead contact—Further information and requests for resources and reagents should be directed to and will be fulfilled by the lead contact: K Venuprasad (venuprasad.poojary@utsouthwestern.edu).

Materials availability—This work did not generate any unique reagents.

Data and code availability—This paper does not report the original code. All software utilized is freely or commercially available and is listed in the key resources table. All data reported in this paper will be shared by the lead contact upon request.

EXPERIMENTAL MODEL AND SUBJECT DETAILS

Mice—C57BL/6 mice, *Rag1*^{-/-} mice, *Rorc*^{tm1Litt/J} mice, and *CD4*^{cre} mice were purchased from the Jackson Laboratory. *Pak2*^{fl/f} mice were described before (Kosoff et al., 2013). Equal number of male and female mice were used. All mice were housed in micro isolator cages in the barrier facility of the University of Texas Southwestern Medical Center. All experiments were performed in accordance with the guidelines of the Institutional Animal Care and Use Committee of the University of Texas Southwestern Medical Center.

Th17 cell-induced colitis—Naïve CD4⁺ T cells were isolated from spleen and lymph nodes from wild-type, *Pak2*^{fl/f}*CD4*^{Cre} mice or *Rorc*^{-/-} mice using CD4⁺ T cell isolation kit. Cells were then stained with antibodies against APC-CD25 and FITC-CD4 and were sorted for CD4⁺CD25⁻ populations (Kumar et al., 2021a). CD4⁺CD25⁻ cells from *Rorc*^{-/-} mice (male and female, 7–8 week old) were lentivirally transduced with ROR γ t and ROR γ t phospho mutants (S316A and S316D) for 24 h. Transduced cells were then cultured under Th17 inducing conditions for 5 days. *Rag1*^{-/-} mice (male and female, 7–8 week old) were injected intra-peritoneally with 5×10^5 Th17 cells and monitored for disease severity up to 8 weeks.

METHOD DETAILS

Plasmid construction and cell transfection—Myc-Itch, HA-Ub (wild-type), and Flag-mROR γ t have been described (Kathania et al., 2016). Transient transfection of 293T cells was performed using Lipofectamine 2000 (Invitrogen) according to the manufacturer's instructions. Myc-Pak2 and Myc-Pak2-K278R were created and cloned into pCDNA3.1 between *NotI* and *BamHI* sites. The sequences of all clones were verified.

Lentiviral transduction—Expression clones were created by Gateway cloning technology according to the manufacturer’s instructions (Invitrogen). Lentiviral expression clones of mouse mROR γ t- S316A, mROR γ t- S316D, Pak2, and Pak2- K278R were constructed by first subcloning into pENTR-3C entry vector (Invitrogen), and then subcloned to pLenti6.2/N-Lumio/V5-DEST (Invitrogen) via Gateway cloning. The ViraPower lentiviral expression system (Invitrogen) was used for packaging and producing lentiviruses in 293FT cells. The supernatant was harvested after 72 h. CD4⁺ T cells were transduced using lentiviruses in the presence of 5 μ g/mL polybrene (Santa Cruz), and the media was changed after 12 h.

Protein identification by liquid chromatography (LC)-tandem MS—The protein samples were processed and analyzed at the Mass Spectrometry Facility of the Department of Pathology at the University of Michigan. Gel slices (10 slices/lane) were destained with 30% methanol for 4 h. Upon reduction (10 mM DTT) and alkylation (65 mM 2-Chloroacetamide) of the cysteines, proteins were digested overnight with sequencing grade, modified trypsin (Promega). The resulting peptides were resolved on a nano-capillary reverse phase column (Acclaim PepMap C18, 2 micron, 25 cm, ThermoScientific) using a 1% acetic acid/acetonitrile gradient at 300 nL/min and directly introduced in to Orbitrap Fusion tribrid mass spectrometer (Thermo Scientific, San Jose CA). MS1 scans were acquired at 120K resolution. Data-dependent high-energy C-trap dissociation MS/MS spectra were acquired with top speed option (3 sec) following each MS1 scan (relative CE ~32%). Proteins were identified by searching the data against the Mus musculus database (24861 entries) using Proteome Discoverer (v1.4, Thermo Scientific). Search parameters included MS1 mass tolerance of 10 ppm and fragment tolerance of 0.2 Da; two missed cleavages were allowed; carbamidimethylation of cysteine was considered fixed modification and oxidation of methionine were considered a potential modification. Percolator algorithm was used for discriminating between correct and incorrect spectrum identification. The false discovery rate (FDR) was calculated at the peptide level and peptides with <1% FDR were retained. Immunoprecipitated proteins were separated by SDS-PAGE. In-gel digestion with trypsin, followed by protein identification using LC-tandem MS, was performed as described elsewhere.⁴³ Briefly, tryptic peptides were resolved on a nano-LC column (Magic AQ C18; Michrom Bioresources, Auburn, CA) and introduced into an Orbitrap mass spectrometer (Thermo Scientific, Waltham, MA). The Orbitrap was set to collect a high-resolution MS1 (FWHM 30,000@400 m/z), followed by the data-dependent collision-induced dissociation spectra on the “top 9” ions in the linear ion trap. Spectra were searched against a human protein database (UniProt release 2011_05) using the X!Tandem/TPP software suite.⁴⁴ Proteins identified with a Protein Prophet probability ≥ 0.9 false discovery rate $\leq 2\%$ were considered for further analysis.

Real-time PCR analysis—Total RNA was prepared using RNeasy Mini Kit (Qiagen), followed by cDNA synthesis using Verso cDNA kit (Thermo Scientific). Quantitative real-time PCR was performed on a Mastercycler Realplex2 (Eppendorf). Light Cycler 480 SYBR Green I master reaction mix (Roche) was used in a 20 μ L reaction volume. The expression of individual genes was normalized to the expression of actin. Cycling conditions were:

95°C for 2 min, followed by 50 cycles of 95°C for 15 sec, 55°C for 15 sec, and 72°C for 20 sec.

Th17 cell differentiation—For *in vitro* experiments, naïve CD4⁺ T cells from the spleen and lymph nodes were differentiated into Th17 cells in plates coated with anti-CD3 (1 µg/mL) and anti-CD28 (2 µg/mL). The cells were cultured in the presence of TGF-β (5 ng/mL), IL-6 (20 ng/mL), anti-IL-4 (5 µg/mL) and anti-IFN-γ (5 µg/mL) antibodies for 5 days.

Flow cytometry—Lamina propria lymphocytes were isolated using the Lamina Propria Dissociation Kit (Miltenyi Biotec) following the manufacturer's instructions. Cells were washed with 1X PBS and then incubated with Fc block (553142, BD Bioscience). Cells were then stained with Live-Dead aqua (L34957, Invitrogen) for live cells and further stained with combinations of antibodies. Antibodies used were Lin-PB (79724, BioLegend), CD45.2-APC (17-0454-81, eBioscience), CD4-FITC (100406, BioLegend), IL-17-PerCP-Cy5.5 (506920, BioLegend), IFN-γ-APC (1554413, BD Bioscience). Data were acquired with a FACSCanto II (BD) and analyzed with FlowJo software (Tree Star).

Immunoprecipitation and immunoblot analysis—Cell lysates were prepared from 293T cells transfected with Myc-Pak2 and Flag-RORγt plasmids after 36 h by homogenizing in NP-40 lysis buffer. Protein estimations were done using the Pierce BCA protein assay kit according to the manufacturer's protocol. Whole-cell lysates were precleared with 20 µL of Protein A/G plus agarose beads (Santa Cruz) for 1 h at 4°C. Lysates were then incubated with 1 µg of the desired antibody overnight at 4°C followed by a further 1 h of incubation at 4°C with 25 µL of Protein A/G beads. The immunocomplexes were washed five times with lysis buffer and denatured using 4X Laemmli buffer. Further, they were separated by SDS-PAGE and immunoblotted with the indicated antibodies. Blots were visualized using Amersham ECL plus immunoblot analysis detection system (GE, Chicago, IL) on a Biorad ChemiDoc. For reprobing, membranes were stripped by incubation in a stripping buffer (62.5 mM Tris-HCl, pH 6.7; 100 mM 2-mercaptoethanol and 2% SDS) at 55°C for 45 min and washed thoroughly before reprobing.

In vitro kinase assays—Pak2 kinase activity was assessed using ADP-Glo Kinase Assay Kit (V9101, Promega), following the manufacturer's instructions. Recombinant RORγt protein (1 µg) was incubated with 100 ng of recombinant Pak2 kinase. The kinase reaction with a final ATP concentration of 50 µM was incubated at room temperature for 2 h. The kinase reaction was then terminated by adding ADP-Glo reagent for 40 min, followed by the addition of kinase detection reagent for 30 min incubation before reading the luminescence on a multimode microplate reader.

Ubiquitination assay—293T cells were transfected with Flag-RORγt, Myc-Itch, and various other constructs as indicated. MG132 was added 6 h before cell lysis. Cells were washed three times with PBS and lysed in NP-40 lysis buffer. Immunoprecipitation was performed using anti-Flag antibody. RORγt-associated ubiquitin was analyzed by immunoblot using antibody against HA. An *in vitro* ubiquitination assay was performed using the E2-Ubiquitin Conjugation Kit (Abcam, Cambridge, MA) with GST-RORγt, GST-

ROR γ t- S316A or GST-ROR γ t- S316D protein as substrate and Itch as the E3 ligase following the manufacturer's protocol.

TUBE pull-down assay—The pull-down of ubiquitinated proteins was performed with GST-tagged TUBE, following the manufacturer's instructions (Life Sensors). Briefly, for Pan-Ub, cells were collected, washed twice with PBS, and lysed with TUBE buffer supplemented with protease inhibitors (Pierce) and 5 mM NEM. Clarified lysates were incubated for 2 h on equilibrated glutathione Sepharose-GST-TUBE under rotation (Mukherjee et al., 2020). The resin was washed 3 times with TBS-T (200 mM Tris-HCl pH 8.0, 0.15 M NaCl, 0.1% Tween-20) and resolved by SDS-PAGE. ROR γ t-associated ubiquitin was analyzed by immunoblot using antibody against HA.

Protein expression and purification—ROR γ t and ROR γ t mutant (S316A and S316D) were sub-cloned into pGEX-6P1-DEST vector containing GST tag at N-terminal. Further, GST-ROR γ t and GST-ROR γ t mutant proteins were individually expressed in RosettaTM(DE3) pLysS *E. coli*. Cleared lysates were prepared and the soluble fusion proteins were purified on glutathione Sepharose 4B GST-tagged protein purification resin (GE Healthcare Life Sciences) and tested by immunoblot using monoclonal anti-GST (Cell Signaling Technology). GST-Itch protein was purified as shown previously (Paul et al., 2018).

Homology modeling—The protein sequences of mouse ROR γ t were retrieved from the UniProt database (P51450-2). Homologs to the target mouse ROR γ t LBD domain sequence were identified by PSI-blast for PDB databank on NCBI. The three-dimensional structure of mouse ROR γ t LBD domain was generated by SWISS-MODEL using the PDB: 5EJV. The substitution mutation of S316 to D316 was performed in PyMol. H-bond distances between the amino acids were measured in PyMol. Further, the analysis of the modeled structure of the LBD domain of mouse ROR γ t by AlphaFold (AF-P51450-F1) was done in PyMol.

Colonoscopic examination—To measure colitis severity, a high-resolution murine video endoscopic system was used. For monitoring colon inflammation *in vivo*, mice were anesthetized with Ketamine/Xylazine, and endoscopy was performed using a mini-endoscope from Karl-Storz. Grading of colitis scores was performed according to the mouse endoscopic index of colitis severity (MEICS). In brief, MEICS was determined by perianal findings, wall transparency, intestinal bleeding, and focal lesion. Each of these four different parameters of inflammation was given a score from 0 to 3, resulting in a total MEICS ranging from 0 to 12 (Kodani et al., 2013).

QUANTIFICATION AND STATISTICAL ANALYSIS

Data are represented as mean \pm SD. Differences in group survival were analyzed by the Kaplan-Meier test using Prism 8 (GraphPad Software). Statistical significance was determined by unpaired Student's t-test and one-way ANOVA; $p < 0.05$ was considered statistically significant.

Supplementary Material

Refer to Web version on PubMed Central for supplementary material.

ACKNOWLEDGMENTS

The authors thank Dr. Ezra Burstein for the helpful discussions. This work was supported by funds from the National Institutes of Health (R01-DK115668 and R01-AI155786) and Cancer Prevention Research Institute of Texas (RP160577 and RP190527), a translational pilot project grant from the Harold C. Simmons Comprehensive Cancer Center, UT Southwestern Medical Center (23001045) to K.V., and R01-DK117001 to K.V. and A.L.T.

REFERENCES

- Beringer A, Noack M, and Miossec P (2016). IL-17 in chronic inflammation: from discovery to targeting. *Trends Mol. Med* 22, 230–241. 10.1016/j.molmed.2016.01.001. [PubMed: 26837266]
- Chong WP, Mattapallil MJ, Raychaudhuri K, Bing SJ, Wu S, Zhong Y, Wang W, Chen Z, Silver PB, Jittayasothorn Y, et al. (2020). The cytokine IL-17A limits Th17 pathogenicity via a negative feedback loop driven by Auto-crine induction of IL-24. *Immunity* 53, 384–397.e5. 10.1016/j.immuni.2020.06.022. [PubMed: 32673565]
- Duerr RH, Taylor KD, Brant SR, Rioux JD, Silverberg MS, Daly MJ, Steinhart AH, Abraham C, Regueiro M, Griffiths A, et al. (2006). A genome-wide association study identifies IL23R as an inflammatory bowel disease gene. *Science* 314, 1461–1463. 10.1126/science.1135245. [PubMed: 17068223]
- Fitzpatrick LR (2013). Inhibition of IL-17 as a pharmacological approach for IBD. *Int. Rev. Immunol* 32, 544–555. 10.3109/08830185.2013.821118. [PubMed: 23886112]
- Fragoulis GE, Siebert S, and McInnes IB (2016). Therapeutic targeting of IL-17 and IL-23 cytokines in immune-mediated diseases. *Annu. Rev. Med* 67, 337–353. 10.1146/annurev-med-051914-021944. [PubMed: 26565676]
- Gaffen SL (2009). Structure and signalling in the IL-17 receptor family. *Nat. Rev. Immunol* 9, 556–567. 10.1038/nri2586. [PubMed: 19575028]
- Genovese MC, Durez P, Richards HB, Supronik J, Dokoupilova E, Mazurov V, Aelion JA, Lee SH, Coddling CE, Kellner H, et al. (2013). Efficacy and safety of secukinumab in patients with rheumatoid arthritis: a phase II, dose-finding, double-blind, randomised, placebo controlled study. *Ann. Rheum. Dis* 72, 863–869. 10.1136/annrheumdis-2012-201601. [PubMed: 22730366]
- Ha BH, Morse EM, Turk BE, and Boggon TJ (2015). Signaling, regulation, and specificity of the type II p21-activated kinases. *J. Biol. Chem* 290, 12975–12983. 10.1074/jbc.R115.650416. [PubMed: 25855792]
- Honda K, and Littman DR (2016). The microbiota in adaptive immune homeostasis and disease. *Nature* 535, 75–84. 10.1038/nature18848. [PubMed: 27383982]
- Hueber W, Patel DD, Dryja T, Wright AM, Koroleva I, Bruin G, Antoni C, Draelos Z, Gold MH, et al. ; Psoriasis Study Group (2010). Effects of AIN457, a fully human antibody to interleukin-17A, on psoriasis, rheumatoid arthritis, and uveitis. *Sci. Transl. Med* 2, 52ra72. 10.1126/scitranslmed.3001107.
- Hueber W, Sands BE, Lewitzky S, Vandemeulebroecke M, Reinisch W, Higgins PDR, Wehkamp J, Feagan BG, Yao MD, Karczewski M, et al. (2012). Secukinumab, a human anti-IL-17A monoclonal antibody, for moderate to severe Crohn's disease: unexpected results of a randomised, double-blind placebo-controlled trial. *Gut* 61, 1693–1700. 10.1136/gutjnl-2011-301668. [PubMed: 22595313]
- Hunter T (2007). The age of crosstalk: phosphorylation, ubiquitination, and beyond. *Mol. Cell* 28, 730–738. 10.1016/j.molcel.2007.11.019. [PubMed: 18082598]
- Ivanov II, McKenzie BS, Zhou L, Tadokoro CE, Lepelley A, Lafaille JJ, Cua DJ, and Littman DR (2006). The orphan nuclear receptor ROR-gamma directs the differentiation program of proinflammatory IL-17+ T helper cells. *Cell* 126, 1121–1133. 10.1016/j.cell.2006.07.035. [PubMed: 16990136]

- Kathania M, Khare P, Zeng M, Cantarel B, Zhang H, Ueno H, and Venuprasad K (2016). Itch inhibits IL-17-mediated colon inflammation and tumor-igenesis by ROR-gammat ubiquitination. *Nat. Immunol* 17, 997–1004. 10.1038/ni.3488. [PubMed: 27322655]
- Kodani T, Rodriguez-Palacios A, Corridoni D, Lopetuso L, Di Martino L, Marks B, Pizarro J, Pizarro T, Chak A, and Cominelli F (2013). Flexible colonoscopy in mice to evaluate the severity of colitis and colorectal tumors using a validated endoscopic scoring system. *J. Vis. Exp.*, e50843. 10.3791/50843. [PubMed: 24193215]
- Korn T, Bettelli E, Oukka M, and Kuchroo VK (2009). IL-17 and Th17 cells. *Annu. Rev. Immunol* 27, 485–517. 10.1146/annurev.immunol.021908.132710. [PubMed: 19132915]
- Kosoff R, Chow HY, Radu M, and Chernoff J (2013). Pak2 kinase restrains mast cell FcεpsilonRI receptor signaling through modulation of Rho protein guanine nucleotide exchange factor (GEF) activity. *J. Biol. Chem* 288, 974–983. 10.1074/jbc.M112.422295. [PubMed: 23204526]
- Kumar R, Singh AK, Starokadomskyy P, Luo W, Theiss AL, Burstein E, and Venuprasad K (2021a). Cutting edge: hypoxia-induced Ubc9 promoter hypermethylation regulates IL-17 expression in ulcerative colitis. *J. Immunol* 206, 936–940. 10.4049/jimmunol.2000015. [PubMed: 33504619]
- Kumar R, Theiss AL, and Venuprasad K (2021b). RORgammat protein modifications and IL-17-mediated inflammation. *Trends Immunol.* 42, 1037–1050. 10.1016/j.it.2021.09.005. [PubMed: 34635393]
- Lee YK, Turner H, Maynard CL, Oliver JR, Chen D, Elson CO, and Weaver CT (2009). Late developmental plasticity in the T helper 17 lineage. *Immunity* 30, 92–107. 10.1016/j.immuni.2008.11.005. [PubMed: 19119024]
- Lock C, Hermans G, Pedotti R, Brendolan A, Schadt E, Garren H, Langer-Gould A, Strober S, Cannella B, Allard J, et al. (2002). Gene-microarray analysis of multiple sclerosis lesions yields new targets validated in autoimmune encephalomyelitis. *Nat. Med* 8, 500–508. 10.1038/nm0502-500. [PubMed: 11984595]
- McGeachy MJ, Cua DJ, and Gaffen SL (2019). The IL-17 family of cytokines in Health and disease. *Immunity* 50, 892–906. 10.1016/j.immuni.2019.03.021. [PubMed: 30995505]
- Mukherjee S, Kumar R, Tsakem Lenou E, Basrur V, Kontoyiannis DL, Ioakeimidis F, Mosialos G, Theiss AL, Flavell RA, and Venuprasad K (2020). Deubiquitination of NLRP6 inflammasome by Cyld critically regulates intestinal inflammation. *Nat. Immunol* 21, 626–635. 10.1038/s41590-020-0681-x. [PubMed: 32424362]
- O’Hagan KL, Miller SD, and Phee H (2017). Pak2 is essential for the function of Foxp3+ regulatory T cells through maintaining a suppressive Treg phenotype. *Sci. Rep* 7, 17097. 10.1038/s41598-017-17078-7. [PubMed: 29213081]
- Parkes M, Cortes A, van Heel DA, and Brown MA (2013). Genetic insights into common pathways and complex relationships among immune-mediated diseases. *Nat. Rev. Genet* 14, 661–673. 10.1038/nrg3502. [PubMed: 23917628]
- Patel DD, and Kuchroo VK (2015). Th17 cell pathway in human immunity: lessons from genetics and therapeutic interventions. *Immunity* 43, 1040–1051. 10.1016/j.immuni.2015.12.003. [PubMed: 26682981]
- Paul J, Singh AK, Kathania M, Elviche TL, Zeng M, Basrur V, Theiss AL, and Venuprasad K (2018). IL-17-driven intestinal fibrosis is inhibited by Itch-mediated ubiquitination of HIC-5. *Mucosal Immunol.* 11, 427–436. 10.1038/mi.2017.53. [PubMed: 28612841]
- Sato M, Matsuda Y, Wakai T, Kubota M, Osawa M, Fujimaki S, Sanpei A, Takamura M, Yamagiwa S, and Aoyagi Y (2013). P21-activated kinase-2 is a critical mediator of transforming growth factor-beta-induced hepatoma cell migration. *J. Gastroenterol. Hepatol* 28, 1047–1055. 10.1111/jgh.12150. [PubMed: 23425030]
- Sun J, Jia H, Bao X, Wu Y, Zhu T, Li R, and Zhao H (2021). Tumor exosome promotes Th17 cell differentiation by transmitting the lncRNA CRNDE-h in colorectal cancer. *Cell Death Dis.* 12, 123. 10.1038/s41419-020-03376-y. [PubMed: 33495437]
- Taglieri DM, Ushio-Fukai M, and Monasky MM (2014). P21-activated kinase in inflammatory and cardiovascular disease. *Cell. Signal* 26, 2060–2069. 10.1016/j.cellsig.2014.04.020. [PubMed: 24794532]

- Targan SR, Feagan B, Vermeire S, Panaccione R, Melmed GY, Landers C, Li D, Russell C, Newmark R, Zhang N, et al. (2016). A randomized, double-blind, placebo-controlled phase 2 study of brodalumab in patients with moderate-to-severe Crohn's disease. *Am. J. Gastroenterol* 111, 1599–1607. 10.1038/ajg.2016.298. [PubMed: 27481309]
- Venuprasad K, Zeng M, Baughan SL, and Massoumi R (2015). Multifaceted role of the ubiquitin ligase Itch in immune regulation. *Immunol. Cell Biol* 93, 452–460. 10.1038/icb.2014.118. [PubMed: 25582340]
- Wilkes MC, and Leof EB (2006). Transforming growth factor beta activation of c-Abl is independent of receptor internalization and regulated by phosphatidylinositol 3-kinase and PAK2 in mesenchymal cultures. *J. Biol. Chem* 281, 27846–27854. 10.1074/jbc.M603721200. [PubMed: 16867995]
- Wilkes MC, Mitchell H, Penheiter SG, Doré JJ, Suzuki K, Edens M, Sharma DK, Pagano RE, and Leof EB (2005). Transforming growth factor-beta activation of phosphatidylinositol 3-kinase is independent of Smad2 and Smad3 and regulates fibroblast responses via p21-activated kinase-2. *Cancer Res.* 65, 10431–10440. 10.1158/0008-5472.CAN-05-1522. [PubMed: 16288034]
- Wilkes MC, Murphy SJ, Garamszegi N, and Leof EB (2003). Cell-type-specific activation of PAK2 by transforming growth factor beta independent of Smad2 and Smad3. *Mol. Cell Biol* 23, 8878–8889. 10.1128/MCB.23.23.8878-8889.2003. [PubMed: 14612425]
- Wilkes MC, Repellin CE, Hong M, Bracamonte M, Penheiter SG, Borg JP, and Leof EB (2009). Erbin and the NF2 tumor suppressor Merlin cooperatively regulate cell-type-specific activation of PAK2 by TGF-beta. *Dev. Cell* 16, 433–444. 10.1016/j.devcel.2009.01.009. [PubMed: 19289088]
- Yan X, Zhang J, Sun Q, Tuazon PT, Wu X, Traugh JA, and Chen YG (2012). p21-Activated kinase 2 (PAK2) inhibits TGF-beta signaling in Madin-Darby canine kidney (MDCK) epithelial cells by interfering with the receptor-Smad interaction. *J. Biol. Chem* 287, 13705–13712. 10.1074/jbc.M112.346221. [PubMed: 22393057]
- Zhang F, Meng G, and Strober W (2008). Interactions among the transcription factors Runx1, RORgammat and Foxp3 regulate the differentiation of interleukin 17-producing T cells. *Nat. Immunol* 9, 1297–1306. 10.1038/ni.1663. [PubMed: 18849990]
- Zhou W, and Sonnenberg GF (2020). Activation and suppression of group 3 innate lymphoid cells in the gut. *Trends Immunol.* 41, 721–733. 10.1016/j.it.2020.06.009. [PubMed: 32646594]

Highlights

- Pak2 directly binds and phosphorylates ROR γ t at S316
- Inhibition of Pak2 in Th17 cells enhances IL-17 expression and colitis severity
- Phosphorylation facilitates binding of Itch to ROR γ t and promotes its degradation

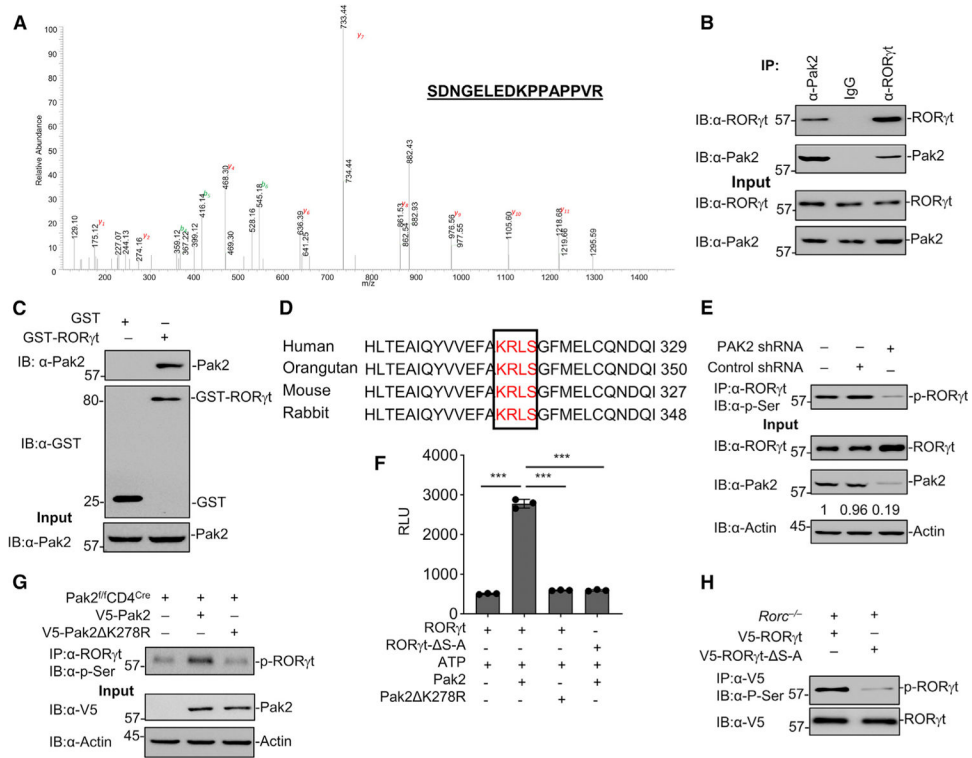


Figure 1. Pak2 interacts and phosphorylates RORγt

(A) Lysate of Th17 cells was precipitated using anti-RORγt antibody and subjected to high-resolution liquid chromatography with tandem mass spectrometry (LC-MS/MS) analysis. A representative LC-MS/MS spectrum corresponding to SDNGELEDKPPAPPVR of Pak2 is shown. Observed b and y ions are indicated.

(B) Lysates were prepared from Th17 cells and immunoprecipitated using anti-RORγt and anti-Pak2 antibody analyzed by western blotting with anti-RORγt and anti-Pak2 antibody.

(C) Immunoblotting of recombinant Pak2 precipitated with GST or GST-RORγt. Below are input controls for recombinant Pak2.

(D) Sequence alignment of RORγt showing the conserved KRLS motif.

(E) Pak2 was knocked down in CD4⁺ T cells using shRNA and cultured under Th17-inducing conditions. The cells were restimulated with anti-CD3 and anti-CD28 antibodies, and the lysate was subjected to immunoprecipitation (IP) with anti-RORγt antibody and analyzed by p-Ser specific antibody.

(F) ADP-glow kinase assay result is represented as relative luciferase units (RLUs).

(G) CD4⁺ T cells from *Pak2^{fl}CD4^{Cre}* were reconstituted with either wild-type or kinase-dead mutant of Pak2 and cultured under Th17 condition. Cell lysates were subjected to IP with anti-RORγt antibody and analyzed by p-Ser specific antibody.

(H) CD4⁺ T cells were isolated from *Rorc^{-/-}* mice, reconstituted with either wild-type or RORγt- S316A mutant, and cultured under Th17 condition. Cell lysates were subjected to IP with anti-V5 antibody and analyzed by p-Ser specific antibody.

Data are representative of two independent experiments. Data represent means ± SD. *p < 0.05; **p < 0.01; ***p < 0.001.

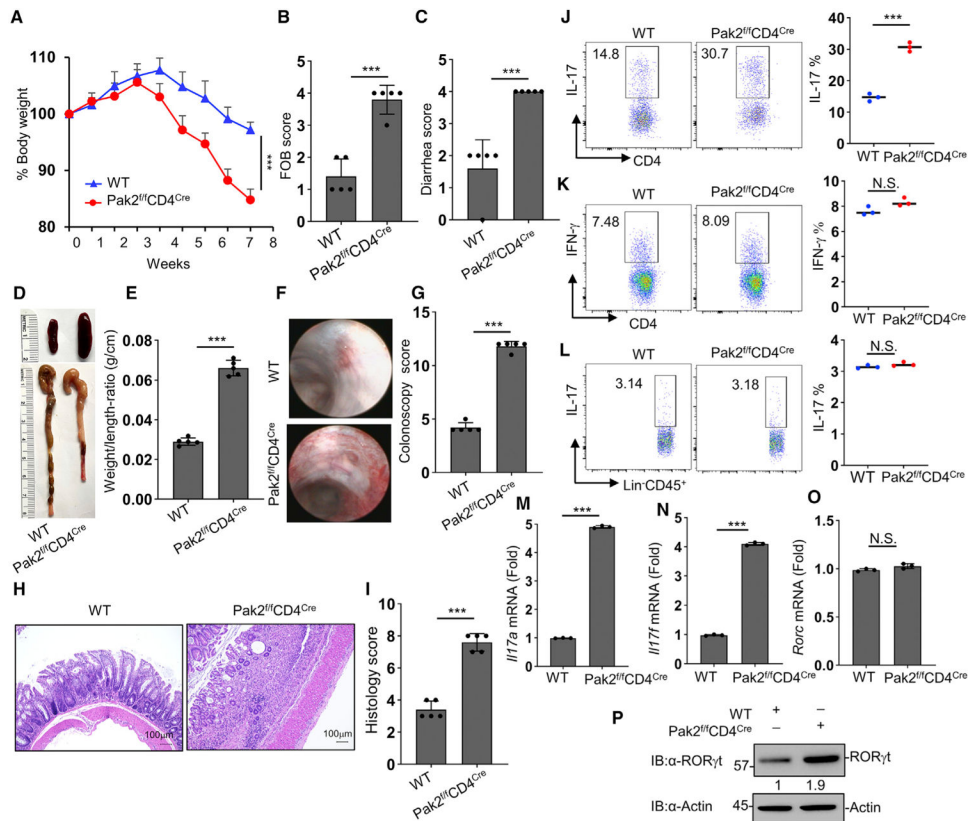


Figure 2. Pak2 inhibition enhances IL-17 expression and Th17 cell-induced colitis

Th17 cells were generated *in vitro* using CD4⁺ T cells isolated from wild-type and *Pak2^{fl/fl}CD4^{Cre}* mice and injected intraperitoneally into *Rag1^{-/-}* mice (n = 5 animals per group).

(A) Body weight change in percentage.

(B) FOB score.

(C) Diarrhea score.

(D) Representative image of colon and spleen.

(E) Colon weight to length ratio.

(F) Representative colonoscopic images.

(G) Colonoscopy score.

(H) Representative H&E images. Scale bars, 100 μ m.

(I) Histology score.

(J and K) cLPLs were stained with anti-CD4, anti-IL-17, and anti-IFN- γ antibodies and analyzed by flow cytometry.

(L) Flow cytometric analysis of IL-17 expression by ILCs in cLPLs.

(M–O) RNA isolated from cLPLs was assayed for the expression of *Il17a*, *Il17f*, and *Rorc* by real-time PCR.

(P) Lysates from CD4⁺ T cells sorted from cLPLs were analyzed by immunoblotting with anti-ROR γ t and anti-actin antibodies.

Data are representative of two independent experiments (n = 5). Dots indicate individual mice. Data represent means \pm SD. *p < 0.05; **p < 0.01; ***p < 0.001. N.S., not significant.

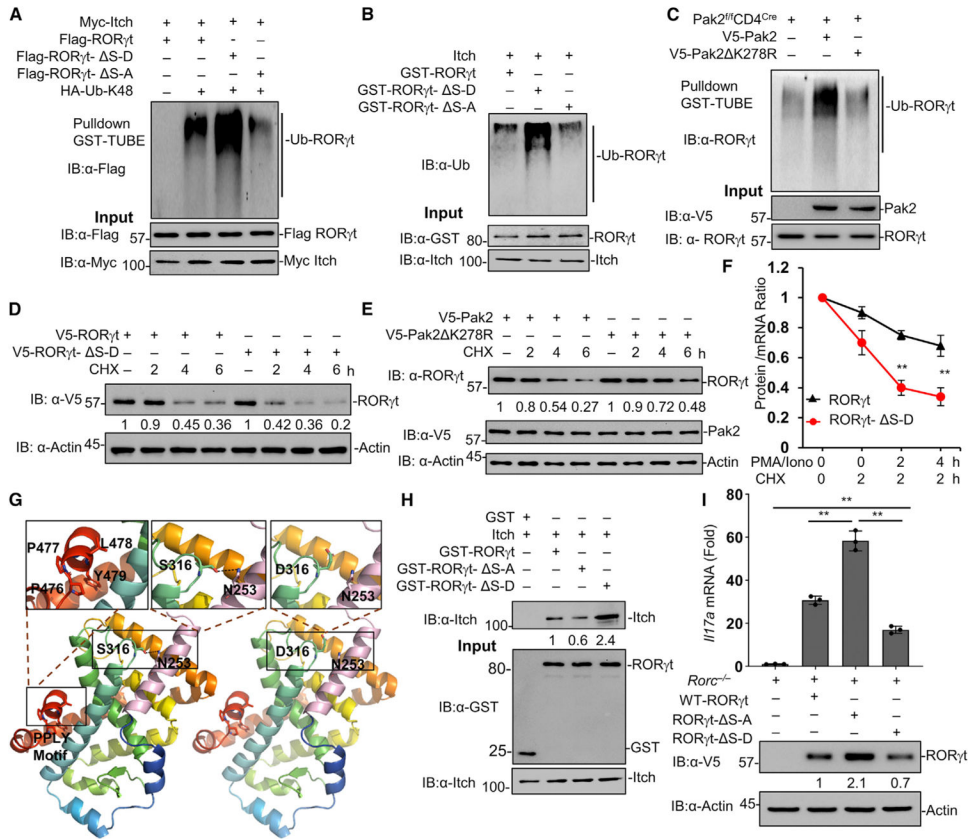


Figure 3. Pak2 enhances the ubiquitination of RORγt and regulates IL-17 expression
 (A) 293T cells were co-transfected with Itch, RORγt, or RORγt mutants. Cell lysates were prepared and subjected to immunoprecipitation using GST-TUBE, followed by immunoblotting analysis with the indicated antibodies.
 (B) *In vitro* ubiquitination of RORγt and RORγt mutants.
 (C) CD4⁺ T cells from *Pak2^{fl/fl}CD4^{Cre}* mice were reconstituted with either wild-type Pak2 or Pak2 K278R mutant and cultured under Th17 condition. Cell lysates were immunoprecipitated using GST-TUBE, followed by immunoblotting with the indicated antibodies.
 (D) CD4⁺ T cells from *Rorc^{-/-}* mice were reconstituted with wild-type RORγt or RORγt-S316D mutant. Cells were treated with cycloheximide (CHX) for the indicated times. Cell lysates were analyzed by immunoblotting with anti-RORγt antibody and anti-actin antibody.
 (E) Th17 cells generated *in vitro* from *Pak2^{fl/fl}CD4^{Cre}* mice were reconstituted with wild-type Pak2 and Pak2 K278R mutant. Cells were treated with CHX for the indicated times. Cell lysates were analyzed by immunoblotting with anti-RORγt antibody, anti-V5, and anti-actin antibody.
 (F) Protein mRNA to ratio of wild-type RORγt and RORγt S316D mutant at indicated time points following stimulation with PMA/ionomycin activation and CHX.
 (G) *In silico* analysis of mutation of S316D on RORγt.
 (H) Immunoblotting of recombinant Itch precipitated with GST, GST-RORγt, or GST-RORγt mutants. Below are input controls for recombinant GST alone, GST-RORγt, GST-RORγt mutants, and Itch.
 (I) IL17a mRNA levels in *Rorc^{-/-}* cells.

(I) CD4⁺ T cells from *Rorc*^{-/-} mice and reconstituted with either wild-type ROR γ t or ROR γ t phospho-mutants. Cells were then cultured under Th17 conditions, and *Il17a* expression was analyzed by real-time PCR. Below is the western blot expression of ROR γ t and ROR γ t phospho-mutants.

Data are representative of three independent experiments. Data represent means \pm SD. *p < 0.05; **p < 0.01; ***p < 0.001. N.S., not significant.

Author Manuscript

Author Manuscript

Author Manuscript

Author Manuscript

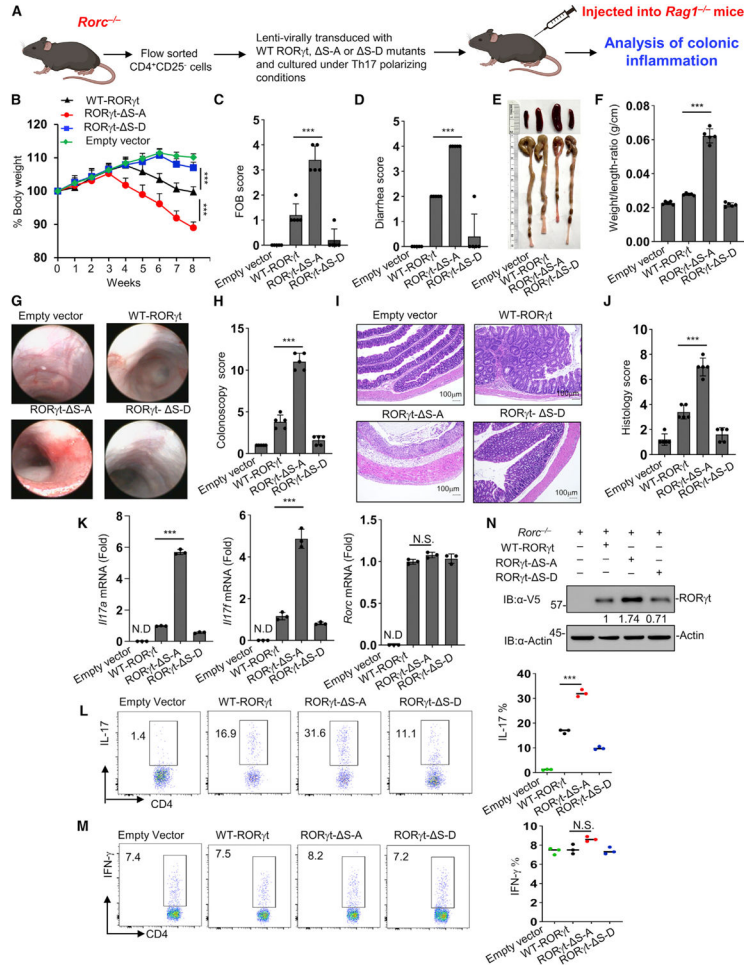


Figure 4. ROR γ t phosphorylation regulates colonic inflammation
 (A) Schematic diagram of Th17 cell-induced colitis model (n = 5 animals per group).
 (B) Body weight change in percentage.
 (C) FOB score.
 (D) Diarrhea score.
 (E) Spleen and colon length.
 (F) Colon weight-to-length ratio.
 (G) Representative colonoscopic images.
 (H) Colonoscopic score.
 (I) Representative H&E images.
 (J) Histology score.
 (K) Real-time PCR analysis of *Il17a*, *Il17f*, and *Rorc*.
 (L and M) Flow cytometric analysis of IL-17 and IFN- γ by adoptively transferred Th17 cells.
 (N) Lysates from cLPLs were analyzed by immunoblotting with anti-ROR γ t and anti-actin antibodies.
 Data are representative of two independent experiments (n = 5). Dots indicate individual mice. Data represent means \pm SD. *p < 0.05; **p < 0.01; ***p < 0.001. N.S., not significant.

KEY RESOURCES TABLE

REAGENT or RESOURCE	SOURCE	IDENTIFIER
Antibodies		
Anti-c-Myc (9E10)	Santa Cruz Biotechnology	Cat: sc-40; RRID:AB_2857941
Anti-Pak2	Santa Cruz Biotechnology	Cat: sc-133113; RRID:AB_1568809
Anti-Flag (M2)	Sigma Aldrich	Cat: F1804; RRID:AB_262044
Anti-ROR γ t (FKJS-9)	eBioscience	Cat:14698882; RRID:AB_1834475
Anti-Itch (32)	BD Bioscience	Cat: 611198; RRID:AB_398732
Anti-ROR γ t (O28-835)	BD Bioscience	Cat: 562197; RRID:AB_10894594
Anti-GST (B14)	Santa Cruz Biotechnology	Cat: sc-138; RRID:AB_627677
Anti-Ahr (B-11)	Santa Cruz Biotechnology	Cat: sc-74571; RRID:AB_2223948
Anti- β -actin(C4)	Santa Cruz Biotechnology	Cat: sc-47778; RRID:AB_626632
Anti-mouse-HRP	Amersham Bioscience	Cat: NA931; RRID:AB_772210
Anti-rabbit-HRP	Cell Signaling Technology	Cat: 7074; RRID:AB_2099233
Clean-Blot™ IP (HRP)	Thermo Fisher Scientific	Cat: 21230; RRID:AB_2864363
Veriblot IP (HRP)	Abcam	Cat: 131366; RRID:AB_2892718
Anti-CD45-APC (104)	eBioscience	Cat:17045482; RRID:AB_469400
Anti-IL17-PerCP-Cy5.5 (TC11)	Biolegend	Cat:506920; RRID:AB_961384
Anti-CD4-FITC (GK1.5)	Biolegend	Cat:100406; RRID:AB_312691
Anti-IFN- γ -APC	BD Bioscience	Cat:554413;RRID:AB_398551
FC-block (2.4G2)	BD Bioscience	Cat:553142; RRID:AB_394657
Anti-mouse CD3e	Biolegend	Cat:100223; RRID:AB_1877072
Anti-mouse IFN- γ	BioXCell	Cat:BE0054; RRID:AB_1107692
Anti-mouse CD28	BioXCell	Cat:BE0015; RRID:AB_1107624
Chemicals, peptides, and recombinant proteins		
Murine IL-2	Peptotech	Cat: 212–12
Murine IL-6	Peptotech	Cat: 216–16B
Murine TGF- β 1	Peptotech	Cat: 100–21
Pak2 shRNA(m) lentiviral particle	Santa Cruz Biotechnology	Cat: sc-36184-V
Live Dead Aqua	Invitrogen	Cat: L34957
Cytofix/Cytoperm	BD Bioscience	Cat: 55028
Perm/Wash Buffer	BD Bioscience	Cat: 554723
Lamina Propria Dissociation Kit (mouse)	Miltenyi Biotec	Cat:130097410
Naive CD4 ⁺ T Cell Isolation Kit (mouse)	Miltenyi Biotec	Cat:130104453
CD4 ⁺ T Cell Isolation Kit (mouse)	Miltenyi Biotec	Cat:130104454
Verso cDNA Synthesis Kit	Thermo Fisher Scientific	Cat: AB1453/B
SYBR GREEN I Master Mix (2X)	Roche Diagnostic	Cat: 507203180
OneTaq 2X Master Mix	NEB	Cat: M0482L
Q5@ Site-Directed Mutagenesis Kit	NEB	Cat: E0554S
QIAGEN Plasmid Plus Maxi Kit	Qiagen	Cat: 12963
QIAquick Gel Extraction Kit	Qiagen	Cat: 28706
RNeasy Micro Kit	Qiagen	Cat: 74004

REAGENT or RESOURCE	SOURCE	IDENTIFIER
RNeasy Mini Kit	Qiagen	Cat: 74104
Luciferase Assay System	Promega	Cat: E1500
LS Columns MACS Separation Columns	Miltenyi Biotec	Cat:130042401
cOmplete™, Protease Inhibitor Cocktail	Roche	Cat:4693159001
Phorbol 12-myristate 13-acetate (PMA)	Sigma Aldrich	Cat: P8139
Phorbol 12-myristate 13-acetate (PMA)	Sigma Aldrich	Cat: P8139
Ionomycin calcium salt	Sigma Aldrich	Cat: I0634
Restore™ Western Blot Stripping Buffer	Thermo Fisher Scientific	Cat: 21063
ECL Prime Detection Reagent	GE Healthcare	Cat: RPN2236
Lipofectamine™ 2000	Thermo Fisher Scientific	Cat:11668019
RPMI 1640 Medium	Thermo Fisher Scientific	Cat:11875093
HBSS	Thermo Fisher Scientific	Cat:14175103
Golgi Stop	BD Bioscience	Cat: 554724
Golgi Plug	BD Bioscience	Cat: 555029
RNase-Free DNase Set	Qiagen	Cat: 79254
RBC Lysis Buffer (10X)	Biolegend	Cat: 420301
SYBR Safe DNA Gel Stain	Invitrogen	Cat: S33102
Protein A/G PLUS-Agarose	Santa Cruz Biotechnology	Cat: sc2003
Experimental models: Cell lines		
HEK293T	ATCC	Cat: CRL-3216
Experimental models: Organisms/strains		
Mouse: C57BL/6	Jackson Laboratory	Cat:000664; RRID:IMSR_JAX:000664
Mouse: <i>Rag1</i> ^{-/-}	Jackson Laboratory	Cat:002216; RRID:IMSR_JAX:002216
Mouse: <i>Pak2</i> ^{fl/fl}	Dr. Jonathan Chernoff	
Mouse: <i>Rorc</i> ^{tm1LinJ}	Jackson Laboratory	Cat:007571; RRID:IMSR_JAX:007571
Mouse: CD4 ^{cre}	Jackson Laboratory	Cat: 022071; RRID:IMSR_JAX:022071
Recombinant DNA		
Plasmid:MIGR-ROR γ t	Addgene	Cat: 24069
Software and algorithms		
FlowJo v10.5.3	BD Bioscience	https://www.flowjo.com
GraphPad Prism v7	GraphPad	https://www.graphpad.com
Biorender	Biorender	https://biorender.com/
PyMol	Schrodinger	https://pymol.org/2/